ANALYTICAL AND EXPERIMENTAL STUDIES ON PENETRATION INTO GEOLOGICAL TARGETS

M. J. Forrestal
D. B. Longcope

Sandia National Laboratories
Albuquerque, NM 87185

L. M. Lee

Ktech Corp.
Albuquerque, NM 87110

ABSTRACT

This paper summarizes some recent analytical and experimental work on penetration into geological targets. Results from several elastic-plastic type theoretical models which predict forces on penetrators for normal impact into dry porous rock, concrete, and sea ice targets are presented and compared with measurements from field tests. Rigid-body acceleration data from newly developed laboratory scale experiments for impact velocities between 0.2 and 1.2 km/s are also presented.

ANALYTICAL MODELS

In recent papers, Forrestal and Longcope [1,2,3] develop several elastic-plastic type theories to predict forces on conical-nosed penetrators. Constitutive target description consists of a linear hydrostat and a Mohr-Coulomb failure criterion with a tension cutoff [4]. Mathematically,

$$p = K\eta \tag{1a}$$

$$\sigma_r - \sigma_\theta = \mu p + \tau_o \quad , \tau_o = (1 - \mu/3)Q \tag{1b}$$

$$\sigma_\theta \geq -Y \tag{1c}$$

where p is hydrostatic pressure, η is volumetric strain, σ_r, σ_θ are radial and circumferential stress components, measured positive in compression, Q is unconfined compressive strength, and Y is tensile strength. As shown in [1,2], these equations provide reasonably accurate data fits to triaxial material test data for dry porous rock, concrete, and sea ice. These analyses use the cylindrical cavity approximation [5] which idealizes the target as thin independent layers normal to the penetration direction and simplifies the problem to one-dimensional wave propagation in the radial direction. Governing equations are subsequently reduced to nonlinear ordinary differential equations with a similarity transformation and solved numerically or in closed form.

Layers of target material are expanded by the penetrator nose which opens a cavity large enough to permit penetration. This expansion produces annular regions of plastic and elastic response. Forrestal and Longcope [1,2,3] develop four target response models; rigid-plastic, elastic-plastic, rigid-cracked-plastic, and elastic-cracked-plastic. The elastic-plastic model is derived first and results show that circumferential target stresses in excess of reported tensile failure values [4] can be developed. To correct for this inadequacy, the rigid-cracked-plastic model is developed. This model has three regions of response; a plastic region next to the penetrator nose, a radially cracked region with circumferential stress set to zero, and a rigid region. As typical with rigid regions in plasticity solutions, particle velocity is taken as zero and the stresses are taken as those from the static solution [6]. For the elastic-cracked-plastic model, the rigid region is replaced by an elastic region.

To calculate penetration resistance, radial stress on the penetrator nose is required as a function of the target material properties, penetrator nose shape, and penetrator axial velocity. As derived in [7], the axial resultant force on a conical nose is given by

$$F = \pi a^2 \sigma_r \tag{2}$$

where a is the radius of the cylindrical afterbody and σ_r is the radial stress on the penetrator nose calculated from the target motion analyses described above. Radial stresses on the penetrator nose from the four response models for a sea ice target with $\rho_o = 0.92$ Mg/m^3, K = 4.0 GPa, $\tau_c = 10.5$ MPa, $\mu = 0$, Poisson's ratio $\nu = 0.27$, and Y = 0.86 MPa are shown in

in Fig. 1. These data and equation (2) can easily be applied to obtain penetrator rigid-body motion. Radial stress curves of the type shown in Fig. 1 are given in [1] for a concrete target and in [2] for a dry porous rock target.

COMPARISON OF PREDICTIONS WITH FIELD TEST DATA

Test results for penetration into pack ice targets located in the Lincoln Sea, near Alert, Northwest Territory, Canada, are reported by Young [8]. The penetrators had total length 1.07 m, outer diameter 70 mm, a conical nose with length 140 mm, and mass 23 kg. Four penetrators were air-dropped and impacted the pack ice layer at V_z = 159 m/s. Onboard accelerometers, signal conditioning equipment, and a transmitter were contained within the penetrators. The transmitter package occupied the aft 18 mm of the penetrator and was stripped from the main penetrator by fins which eventually interacted with the ice target near the surface. Thus, the transmitter remained near the ice surface, remained electrically connected to the main penetrator with a trailing line, and transmitted acceleration-time data to an airborne receiving station. Four deceleration-time records with 1 kHz resolution are presented by Young [8] and one of these records is shown in Fig. 2.

Predictions of rigid-body penetrator decelerations using bounds on the shear strength data are also shown in Fig. 2. From Fig. 1 and equation (2), deceleration is calculated from

$$m \frac{dV_z}{dt} = -F \qquad (3)$$

where m is the penetrator mass. The penetrator strikes the target at V_z = 159 m/s and the calculation starts when the nose is fully embedded. After nose penetration, t > 1 ms, the theory predicts a slight decay. At t = 8 ms, the penetrator has traveled one body length and it is assumed that the transmitter package with mass 3.2 kg has been suddenly removed by the ice crater. This mass change produces the acceleration jumps shown in Fig. 2. After t = 8 ms, the penetrator progresses with mass 19.5 kg and eventually comes to a sudden stop. The sudden deceleration change occurs because a minimum threshold value of radial stress is required to open a cavity and permit penetration. This threshold stress is the quasi-static solution shown in Fig. 1 for V approaching zero.

Comparison of predictions and measurement from a field test into Antelope tuff, a dry porous rock target, at the Sandia Tonopah Test Range, Nevada, is shown in Fig. 3. This penetrator has total length 1.56 m, afterbody diameter 0.156 m, mass 162 kg, and an ogival nose with 6.0 CRH. The previously discussed theories are developed for conical-nosed penetrators, whereas this penetrator has an ogival nose. Data from several hundred soil penetration tests [10] indicate that a 6.0 CRH ogival nose and a conical nose with half apical angle $\phi = \tan^{-1} 0.30$ are nearly equivalent and this is used for the trajectory calculation. For this test the penetrator was propelled with a Davis gun and impacted the Antelope tuff layer at 520 m/s; other test details are reported in [2].

As discussed in [2,9], sliding frictional forces produce an additional source of resistance to penetration and the predictions shown in Fig. 3 include and neglect sliding friction. Frictional resistance is velocity dependent [11] and this mechanism is required in order to qualitatively predict deceleration-time profiles into dry porous rock targets.

LABORATORY SCALE EXPERIMENTS

Recent laboratory experiments were devised [12] in order to complement field test programs and to obtain data at impact velocities beyond the current field test capability. Gas guns are used to accelerate foundry core targets (a simulated soft sandstone) to steady velocities after which the targets impact 20.6 mm diameter penetrators instrumented with piezoelectric accelerometers. Rigid-body acceleration data are recorded for one ogival and two conical nose shapes over impact velocities between 0.2 and 1.2 km/s. Data from these penetration experiments show a departure in the scaling law which relates force to penetrator velocity for all three nose shapes at impact velocities in the neighborhood of 0.5 to 0.6 km/s, which is currently the limiting impact velocity for full scale tests.

Data and a power law fit for a 6.0 CRH nose shape are shown in Fig. 4. Penetration data in Fig. 4 were obtained from experiments conducted on the Air Force Weapons Laboratory 102 mm bore gas gun and the University of Dayton Research Institute 178 mm bore gas gun. Majority of the data were obtained with the 102 mm gun and the experiments with the 178 mm gun were conducted in order to demonstrate that sample size did not significantly affect penetration resistance.

The analytical models discussed previously are elastic-plastic models. However, triaxial test data for the foundry core material [12] indicate no yielding of the material and the existing models are not directly applicable. Work on modeling of the foundry core material and developing a penetration theory for this target material will be conducted in the future. Since empirical models are widely used as predictive tools, the data in Fig. 4 can be described conveniently in the form

$$F = KV^n \quad , 0.5 < V < 1.2 \text{ km/s} \qquad (4)$$

where K = 109, n = 1.29, and F, V have units of kN, km/s. The root mean relative error for the data fit is 0.6 percent.

REFERENCES

1. M. J. Forrestal and D. B. Longcope, "Closed-Form Solutions for Forces on Conical-Nosed Penetrators into Geological Targets With Constant Shear Strength," Mechanics of Materials, Vol. 1, No. 4, Dec. 1982, pp. 285-295.

2. D. B. Longcope and M. J. Forrestal, "Penetration of Targets Described by a Mohr-Coulomb Failure Criterion With a Tension Cutoff," to be published Journal of Applied Mechanics.

3. M. J. Forrestal, "Forces on Conical-Nosed Penetrators Into Targets With Constant Shear Strength," submitted for publication.

4. R. E. Goodman, Introduction to Rock Mechanics, John Wiley and Sons, New York, 1980.

5. R. F. Bishop, R. Hill, and N. F. Mott, "The Theory of Indentation and Hardness Tests," The Proceedings of the Physical Society, Vol. 57, Part 3, pp. 147-159, May 1945.

6. R. Hill, The Mathematical Theory of Plasticity, Clarendon Press, Oxford, 1950.

7. M. J. Forrestal, F. R. Norwood, and D. B. Longcope, "Penetration Into Targets Described by Locked Hydrostats and Shear Strength," International Journal of Solids and Structures, Vol. 17, pp. 915-924, 1981.

8. C. W. Young and L. J. Keck, "An Air-Dropped Sea Ice Penetrometer," SC-DR-71-0729, Sandia Laboratories, Albuquerque, NM, Dec. 1971.

9. M. J. Forrestal and D. E. Grady, "Penetration Experiments for Normal Impact Into Geological Targets," International Journal of Solids and Structures, Vol. 18, No. 3, 1982, pp. 229-234.

10. C. W. Young, "Depth Prediction for Earth Penetrating Projectiles," Journal of Soil Mechanics and Foundation, Division of ASCE, May 1969, pp. 803-817.

11. F. P. Bowden and D. Tabor, "The Friction and Lubrication of Solids," Part II, Chapter 22, Oxford, 1968.

12. M. J. Forrestal, L. M. Lee, B. D. Jenrette, and R. E. Setchell, "Penetration Into Simulated Geological Targets at Impact Velocities Between 0.2 and 1.2 km/s," submitted for publication.

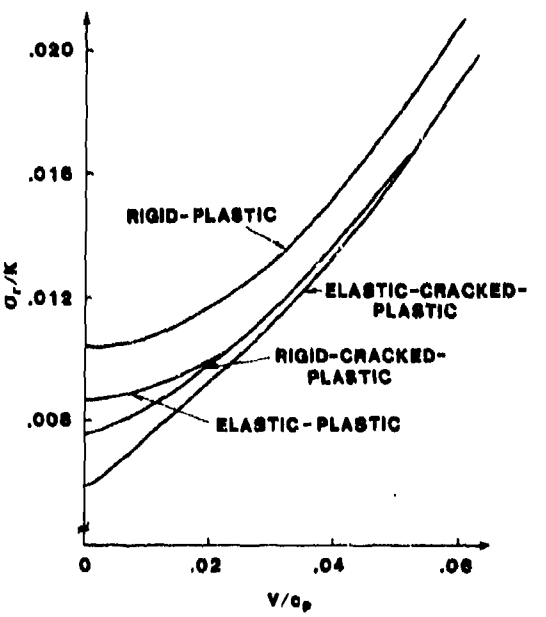

Fig. 1. Radial stress on the penetrator conical nose. $V = V_z \tan \phi$, $c_p^2 = K/\rho_o$ where V_z is axial penetrator velocity and ϕ is the half apical nose angle.

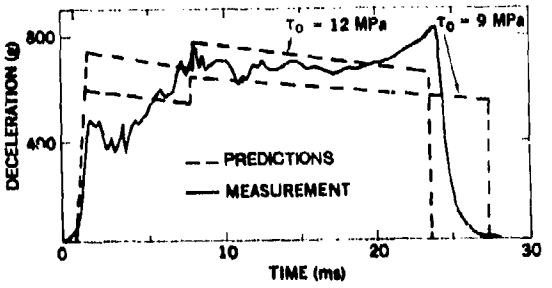

Fig. 2. Deceleration-time measurement and prediction bounds for a sea ice target.

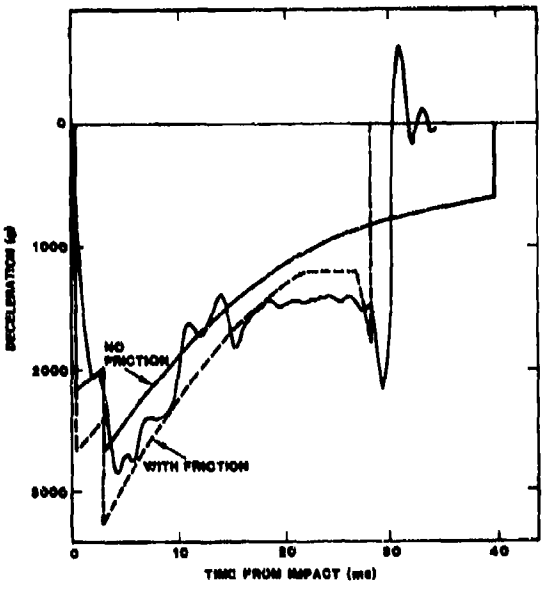

Fig. 3. Deceleration-time measurement and predictions for a dry, porous rock target.

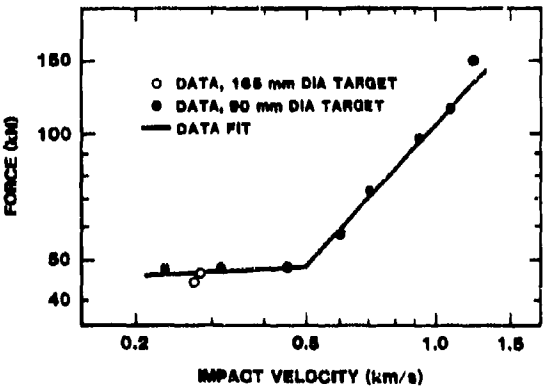

Fig. 4. Laboratory scale data and power law fit for a 6.0 CRH ogival nose.